Manipulation of two-electron states by the electric field in stacked self-assembled dots

2008 J. Phys.: Condens. Matter 20 395225

(http://iopscience.iop.org/0953-8984/20/39/395225)

J. Phys.: Condens. Matter **20** (2008) 395225 (14pp) doi:10.1088/0953-8984/20/39/395225

Manipulation of two-electron states by the electric field in stacked self-assembled dots

M P Nowak[1,2], B Szafran[1] and F M Peeters[2]

[1] Faculty of Physics and Applied Computer Science, AGH University of Science and Technology, aleja Mickiewicza 30, 30-059 Kraków, Poland
[2] Departement Fysica, Universiteit Antwerpen, Groenenborgerlaan 171, B-2020 Antwerpen, Belgium

Received 23 May 2008
Published 4 September 2008
Online at stacks.iop.org/JPhysCM/20/395225

Abstract

A pair of electrons in vertically stacked self-assembled quantum dots is studied and the singlet–triplet energy splitting is calculated in an external electric field using the configuration-interaction method. We show that for double quantum dots the dependence of the singlet energy levels on the electric field involves multiple avoided crossings of three energy levels. The exchange interaction, i.e., the energy difference of the lowest triplet and lowest singlet states, can be tuned by an electric field in a wide range of several tens of meV. For electric fields exceeding a threshold value the exchange interaction becomes a linear function of the field when the two electrons in the singlet state start to occupy the same dot. We also consider non-symmetric confinement, non-perfectly aligned dots, in horizontal as well as vertical field orientation. In a stack of three vertically coupled dots the depth of the confinement in the central dot can be used to enhance the exchange interaction. For a deeper central dot the dependence of the exchange interaction on the electric field is anomalous—it initially decreases when the field is applied in both directions parallel and antiparallel to the axis of the stack. Such a behavior is never observed for a pair of quantum dots.

(Some figures in this article are in colour only in the electronic version)

1. Introduction

Electrons confined in coupled semiconductor quantum dots [1] form orbitals which can be of extended—molecular or localized—ionic character depending on the geometry of the system, the interdot tunnel barrier thickness, and the applied external fields. For two-electron states the character of electron orbitals influences the exchange interaction [2], defined as the difference between the lowest singlet and the lowest triplet energy levels ($J = E_t - E_s$). In the absence of the external magnetic field the energy of the lowest singlet [3–7] is lower that of the lowest triplet unless the electrons occupy separate spatial locations, when the singlet–triplet degeneracy is obtained. The energy of the exchange interaction is a result of a competition between the tunnel coupling, which prevents the spatial separation of electrons, and the electron–electron repulsion which pushes the electrons apart.

The exchange interaction energy is an important quantity for quantum information processing that is based on spins of electrons which are confined in an array of quantum dots [9]. In the model device [9] single spin rotations are performed through a site-selective Rabi oscillation which is induced by an external microwave radiation field. Two-qubit operations are performed through controllable coupling of pairs of electrons by tuning the height of the interdot barrier [2]. The most advanced candidate for the implementation of the spin quantum gate is the multiple-dot system realized in a gated two-dimensional electron gas [10], in which the interdot barrier is controlled by one of the gates which can turn the exchange interaction on and off.

The exchange interaction should be as strong as possible to allow for operation times shorter than the decoherence time. The dots defined in the two-dimensional electron gas have a large spacial extent; consequently it is intrinsically difficult to strongly couple spins of electrons in a pair of such large quantum dots. Even when the interdot barrier is completely removed the electrons are likely to form a Wigner molecule in the single merged dot. In Wigner molecules the confined charge crystallizes in the form of separated single-electron islands resulting in singlet–triplet degeneracy [8]. According to a realistic model of double gated quantum dots the exchange energy is only of the order of 0.1 meV [11]. Optimization of

the interaction energy for laterally coupled dots has been the topic of a number of recent theoretical papers [5, 12, 13].

In this paper we discuss the exchange interaction of two and three vertically stacked self-assembled dots in an external electric field. In stacked self-assembled dots the interdot tunnel barrier is fixed at the growth stage. However, as we discuss below, it is still possible to switch the exchange interaction on and off by applying on electric field parallel to the axis of the device. The exchange energies that we obtain for vertically stacked quantum dots are two orders of magnitude larger than the ones obtained earlier [11] for laterally coupled dots. Such self-assembled dots are attractive for spin manipulation due to the huge single-electron energy spacings of the order of tens of meV, since the rotation of a single spin by the microwave radiation should preferably leave the spatial states unperturbed, i.e. without admixtures of higher excited states. Moreover, the theory on coupled spin qubit operations [9, 2] is based on the Heisenberg Hamiltonian $H_s(t) = J(t)\mathbf{S}_1 \cdot \mathbf{S}_2$. The latter is in fact a low-energy approximation assuming that the excited states have higher energy than the lowest triplet and the lowest singlet energy levels. For instance the two spins as described by the Heisenberg Hamiltonian are swapped within the time τ of the high J pulse such that $\int_0^\tau \mathrm{d}t\, J(t) = \hbar\pi$. When more than two states are involved in the spin exchange operation, the time evolution of the system becomes complex [14] and the exact duration of the on-state of the swap interaction necessary for the spin exchange is difficult to predict. Due to the large energy level spacings the coupled self-assembled dots best satisfy the approximations underpinning Heisenberg Hamiltonian.

Vertically stacked self-assembled quantum dots in external electric fields have recently become a very active research field both experimentally [15, 16] and theoretically [17, 18] in the context of photoluminescence measurements of exciton recombination. The three-dimensional model of coupled quantum dots and the configuration-interaction scheme for diagonalization of the two-particle Hamiltonian that we use here have been previously applied [18] to the Stark effect in double dots. In the photoluminescence experiments the spectral lines exhibit characteristic avoided crossings, which on the one hand are due to hybridization of the single-particle orbitals by the field and on the other hand are related to the transfer of the particles between the dots [18]. The behavior of the electron pair in the external field that we describe in this paper can also be understood as due to avoided crossings that occur separately for the spin-singlet and spin-triplet energy levels. The applied model allows for the description of systems that are not perfectly aligned and for an arbitrary orientation of the electric field, since no symmetry of the system is assumed. We also discuss the singlet and triplet energy levels in a stack containing three quantum dots.

The exchange interaction in a vertical configuration of quantum dots was previously studied [19] for gated structures formed from etched double semiconductor quantum wells. In these double quantum dots the lateral confinement is of electrostatic origin and has a nearly parabolic form, which is different from the quantum well-type confinement found in self-assembled dots. For the electrostatic potential [19] the in-plane electric field orientation (which we also consider in the present work) is irrelevant for the low-energy part of the spectrum, since it only shifts the origin of the harmonic oscillator potential. Moreover, in vertical gated dots the energy spacings between the single-electron energy levels are of the order of 5 meV which is about ten times smaller than in the system discussed here. The huge spacing between the single-electron energy levels that we encounter in self-assembled dots makes the role of the Pauli exclusion much more pronounced than in both vertical gated and laterally coupled dots. For all the structures, the probability to find both electrons in the same dot is larger in the singlet than in the triplet state. This effect can be used to enhance the exchange interaction considerably by introducing intentional asymmetry in the double-dot system [5]. For stacked self-assembled dots it is almost impossible for electrons to occupy the same dot in the triplet configuration at least in the range of electric fields that we consider below.

2. Theory

The confinement potential of a single dot is modeled using a disk quantum well model of depth V_0, diameter R and height $2Z$

$$W(\mathbf{r}; X, \zeta; V_0) = -V_0 \Bigg/ \left[\left(1 + \left(\frac{(x-X)^2 + y^2}{R^2}\right)^{10}\right) \times \left(1 + \left(\frac{(z-\zeta)^2}{Z^2}\right)^{10}\right)\right], \quad (1)$$

where the center of the quantum well is placed at the point $x = X$, $y = 0$ and $Z = \zeta$. The geometrical parameters of a single dot is borrowed from the experiment of [15] in which manipulation of electrons and holes by an electric field was realized. Namely we assume that the dots have diameter $2R = 20$ nm and height $2Z = 4$ nm. The depth of the quantum well $V_0 = 508$ meV is taken for a $In_{0.66}Ga_{0.34}As$ quantum dot [18] embedded in GaAs (we also use the electron effective mass $m = 0.037m_0$, the dielectric constant $\epsilon_0 = 12.5$ for this alloy). In a quantum dot with parameters listed above the single-electron ground-state energy is about -255 meV, i.e. as high as 253 meV above the bottom of the well. The first excited state in this potential is the two-fold degenerate p energy level (angular momentum $\pm\hbar$), whose energy is equal to -187 meV. Therefore, the basic electron excitation in this potential has energy $\Delta E = 68$ meV (for a 2D infinite well of $R = 10$ nm, $\Delta E = 92$ meV is obtained). The spacings between the states is much larger than the interaction energy. For a single dot the interaction energy of two electrons in the ground-state is about 23 meV. Therefore, for multiple dots the wavefunctions for interacting electrons are predominantly constructed from the single-dot ground-state wavefunctions[3]. Nevertheless, the two-electron eigenstates are diagonalized in a basis that includes not only p but also d orbitals (in fact the basis contains 8 localized states per dot, see below).

[3] Note that for ideally aligned dots $s = 0$ and the electric field applied in the growth direction the two-electron states possess a definite angular momentum. Only double lateral excitations (one electron in $l = 1$ and the other in $l = -1$ state) can contribute to the wavefunctions of the low-energy part of the spectrum that always corresponds to $l = 0$.

The confinement potential of multiple dots is taken as a sum of single-dot potentials. Figure 1 shows the cross section of the confinement potential through the $y = 0$ plane for such a pair of quantum dots, whose axes (dashed vertical lines) are separated by $s = 5$ nm with a tunnel barrier between the dots of thickness $b = 6$ nm (the centers of the dots are spaced in the vertical direction by $2Z + b$). The dots are assumed to be identical in size and shape. A different confinement of the dots is introduced through a potential well depth variation. The depth variation is always small compared to the depth of the confinement potential wells. For instance the actual potential plotted in figure 1 was obtained as a sum $V(\mathbf{r}) = W(\mathbf{r}; 0, 10\text{ nm}, V_0) + W(\mathbf{r}; 5\text{ nm}, 0, V_0 + \mathrm{d}V)$ with $\mathrm{d}V = 20$ meV (the lower dot is assumed deeper in this plot).

We consider the Hamiltonian

$$H = h_1 + h_2 + \frac{e^2}{4\pi\epsilon\epsilon_0|\mathbf{r}_{12}|} + |e|\mathbf{F}\cdot(\mathbf{r}_2 + \mathbf{r}_1 - 2\mathbf{r}_\mathbf{x}), \quad (2)$$

where $\mathbf{F}$ is the electric field vector and $\mathbf{r}_x$ is point in which zero electrostatic potential is assumed, h_1 and h_2 are the single-electron energy operators, with

$$h_{1(2)} = -\frac{\hbar^2}{2m^*}\nabla^2_{1(2)} + V(\mathbf{r}_{1(2)}). \quad (3)$$

For the discussion of the results that follow it is convenient to localize $\mathbf{r}_x$ at the plane that passes through the center of the lower dot exactly between the axes of the dots (see the point marked by the star in figure 1). The eigenproblem for operator H is solved using the configuration-interaction method with the variational wavefunction constructed of (anti)symmetrized products of single-electron wavefunctions

$$\Psi(\mathbf{r}_1, \mathbf{r}_2) = \sum_{ij} c_{ij}\,(1 \pm P_{12})\,f_i\,(\mathbf{r}_1)\,f_j(\mathbf{r}_2), \quad (4)$$

where f_i is the ith single-electron wavefunction, P_{12} is the particle exchange operator and we take the $+$ sign for singlets (symmetric spatial function) and $-$ for triplets (antisymmetric spatial function). The single-electron wavefunctions are obtained via diagonalization of Hamiltonian h_1 in a basis of Gaussian functions

$$f_j(\mathbf{r}_p) = \sum_i d_i^{(j)} \exp\left[-\alpha_i\left((x - x_i)^2 + (y - y_i)^2\right) - \beta_i(z - z_i)^2\right], \quad (5)$$

where $d_i^{(j)}$ are the linear variational parameters for the jth wavefunction, α_i, β_i are the nonlinear variational parameters describing the localization strength of the i^{th} Gaussian around point (x_i, y_i, z_i). We apply 8 Gaussian centers per dot (see figure 1(b)): two Gaussians are localized in the center of each dot, four Gaussians are placed on a circle around the axis of each dot within the symmetry plane of the dot and an additional two Gaussians are localized at the symmetry axis of the dot. Precise positions of the Gaussians as well as the values of the localization parameters are optimized for the description of the single-electron states in the absence of the field. In the present approach the electric field is accounted for along with the electron–electron interaction only at the stage of the diagonalization of the two-electron Hamiltonians. The single-electron basis obtained for $F = 0$ is flexible enough to account for the electric field effect in the range considered below. Results obtained with this approach are compared below to the results of the finite difference approach and a very good agreement is demonstrated. A Gaussian basis for single-electron wavefunctions is more suitable for diagonalization of the two-electron eigenproblem than the wavefunctions obtained on a mesh of points with the finite difference approach, since it allows for a much faster integration of the interaction matrix elements.

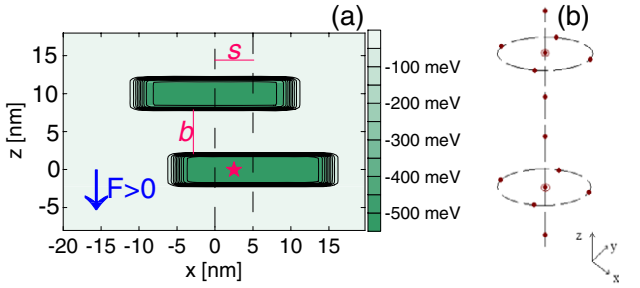

Figure 1. (a) Cross section of the confinement potential for a pair of quantum dots calculated at $y = 0$ plane. Dashed vertical lines show the center of the dots. The height of the vertical barrier is $b = 6$ nm and the dots are displaced by $s = 5$ nm with respect to each other. The lower dot is deeper by 20 meV. The star indicates the zero of the external electric field potential. The arrow indicates the direction of the electric force acting on electrons for $F > 0$. (b) Schematic drawing of the positions of the Gaussian centers in the multicenter basis. The four centers on the two circles are localized within the plane of confinement of each dot. Two Gaussian centers are localized in the center of the dot, and one above and one below the center.

Below, we occasionally refer to the total parity of the two-electron wavefunctions. It is a good quantum number for identical quantum dots, for which $\Psi(I\mathbf{r}_1, I\mathbf{r}_2) = \pm\Psi(\mathbf{r}_1, \mathbf{r}_2)$, where I is the inversion operator with respect to the center of the stack. The wavefunctions which are invariant with respect to this operation have the even total parity, and the ones which change sign have the odd total parity.

3. Results

3.1. Single-electron states

Figure 2(a) shows the electric field dependence of the two lowest energy states for a pair of identical dots separated by a barrier with thickness of $b = 2, 4, 6$ and 11 nm. At $F = 0$ the ground-state wavefunction is a binding orbital, and the first excited state wavefunction is an antibinding orbital (see figure 2). The binding orbital can be constructed as a sum of single-dot wavefunctions

$$\psi_b = \frac{1}{\sqrt{2}}(\psi_1 + \psi_2), \quad (6)$$

where ψ_1 and ψ_2 are the ground-state wavefunctions of the lower and the upper dot assumed both real and non-negative everywhere (the wavefunctions presented in figure 2(d) are

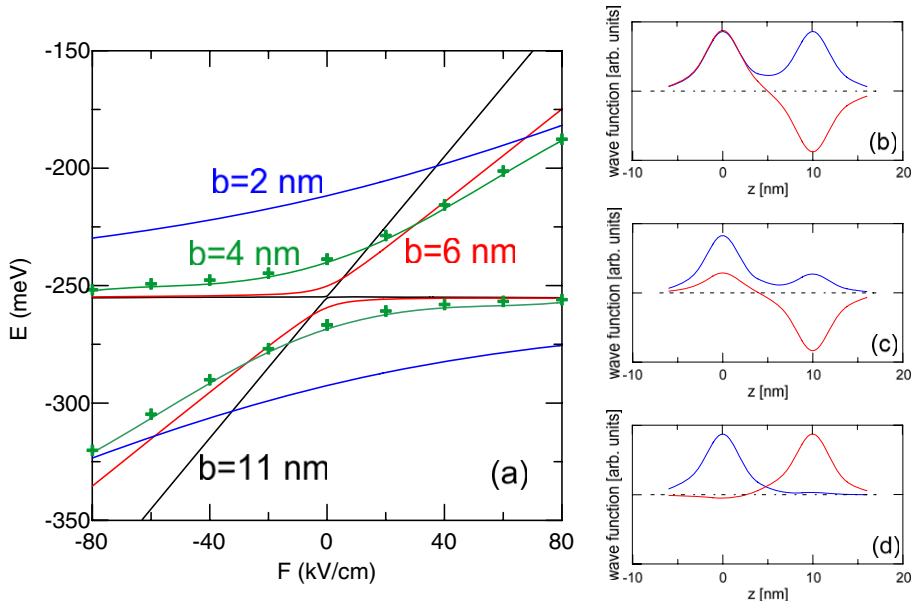

Figure 2. (a) Two lowest energy levels of a single electron in a pair of identical and perfectly aligned dots with the field oriented along the growth direction for $b = 2$, 4, 6 and 11 nm. The crosses show the $b = 4$ nm results as calculated with the finite difference method. Right figures show the binding and antibinding orbitals calculated for $b = 6$ nm. ((b)–(d)) Figures show functions of the ground-state and the first excited state for $F = 0$, 12 and 100 kV cm^{-1}, respectively. Dashed line shows the zero of the wavefunction.

nearly the single-dot wavefunctions). The antibinding orbital is constructed as the difference of the single-dot wavefunctions

$$\psi_a = \frac{1}{\sqrt{2}}(\psi_1 - \psi_2). \tag{7}$$

For $F > 0$ the electric field tends to localize the ground (excited) state in the lower (upper) dot, which results in a reduction of the electron tunnel coupling between the identical dots. The breaking of the tunnel coupling is associated with the avoided crossings of the two energy levels (see figure 2(a)). The width of the avoided crossing is a measure of the electron tunnel coupling strength between the dots. For $b = 2$ nm the energy splitting of the binding and antibinding states is of the order of 100 meV, while for $b = 11$ nm the splitting is only 0.74 meV. In a strong electric field both the ground-state and the first excited state become localized in a single dot (see figures 2(c, d)). Outside the avoided crossing one of the two energy levels becomes almost independent of F (see figure 2(a)). This state is localized within the lower dot, where the electric potential is taken to be zero. At $F \ll 0$ the state localized in the lower dot is the first excited state, and at $F \gg 0$ this state is the ground-state (see figure 2(d)).

The crosses in figure 2(a) show the energy levels as obtained with the finite difference approach for $b = 4$ nm. The results were obtained on a mesh of $43 \times 43 \times 43$ points spaced by 1 nm in each direction using the imaginary time technique [20]. We see that the values agree very well with the ones obtained using the multicenter basis (the solid curves).

3.2. Two-electron states in the absence of the electric field

The low-energy part of the spectrum for the electron pair is plotted in figure 3 as function of the interdot barrier thickness.

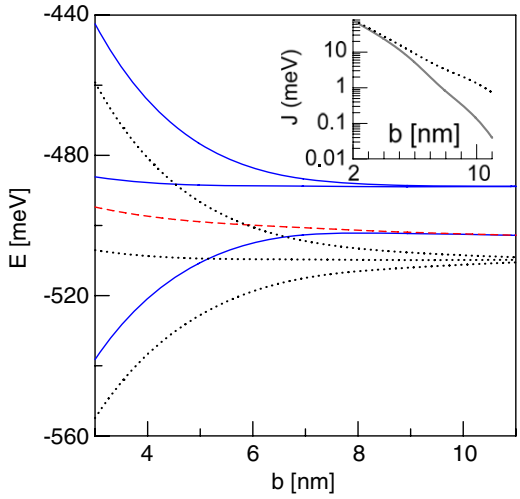

Figure 3. Lowest energy levels for the two-electron system in the case of two perfectly aligned identical dots spaced by a barrier of thickness b. Dotted black curves show the results for non-interacting electrons. The ground-state and the second excited state of the non-interacting system are non-degenerate and correspond to spin-singlets. The first excited state is degenerate and contains a singlet state and a triplet state. Dashed and solid curves correspond to the case of interacting electrons. The dashed curve shows the spin-triplet and the solid lines the spin-singlet. Inset: exchange energy for two interacting electrons (solid line) and for non-interacting electrons (dotted curve).

Dotted curves in figure 3 show the lowest energy levels of the non-interacting system. All the presented non-interacting energy levels tend to degeneracy for large b. For any b, in the absence of electron–electron interaction the ground-state wavefunction is a simple product of single-electron

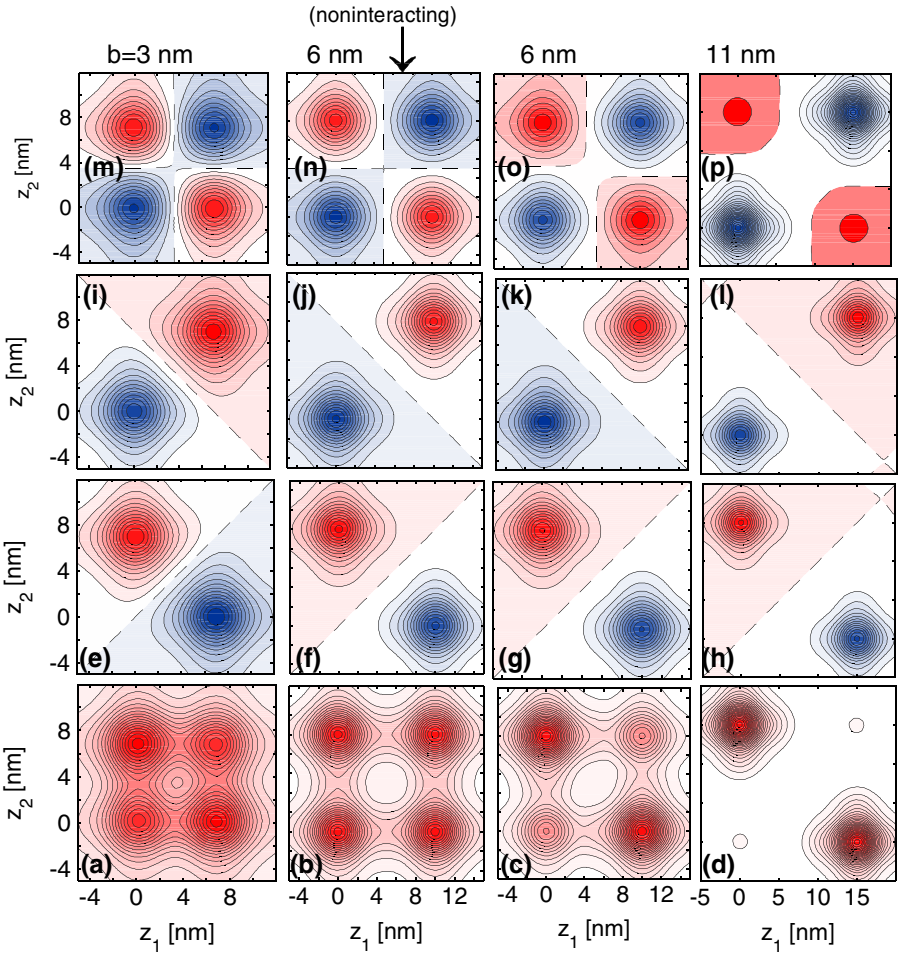

Figure 4. Contour plots of the wavefunction for two electrons in vertically coupled identical quantum dots that are separated by a barrier with thickness $b = 2$, 6 and 11 nm in the absence of an electric field ($F = 0$). Results are shown in the z_1, z_2 plane, the second column shows the results for $b = 6$ nm with neglected electron–electron interaction. Plotted for $y_1 = x_1 = y_2 = x_2 = 0$. Thick dashed lines indicate the zeros of the wavefunction. Plots ((a)–(d)) correspond to the ground-state (spin-singlet with even parity), ((e)–(h)) to the first excited state (spin-triplet with odd parity), ((i)–(l)) to the second excited state (singlet with odd parity) and ((m)–(p)) to the third excited state (singlet with even parity).

binding orbitals

$$\Psi_0(\mathbf{r}_1, \mathbf{r}_2) = \psi_b(\mathbf{r}_1)\psi_b(\mathbf{r}_2). \tag{8}$$

Substituting the definition of the binding orbital we obtain the expression

$$\Psi_0(\mathbf{r}_1, \mathbf{r}_2) = \tfrac{1}{2}\left(\psi_1(\mathbf{r}_1)\psi_1(\mathbf{r}_2) + \psi_2(\mathbf{r}_1)\psi_2(\mathbf{r}_2) + \psi_1(\mathbf{r}_1)\psi_2(\mathbf{r}_2) + \psi_2(\mathbf{r}_1)\psi_1(\mathbf{r}_2)\right). \tag{9}$$

The ground-state wavefunction of the non-interacting pair for $b = 6$ nm is plotted in figure 4(b). The wavefunction is calculated along the axis of the system ($x_1 = y_1 = x_2 = y_2 = 0$) as a function of the vertical coordinates of the two particles. The wavefunction possesses four identical maxima that correspond to electrons localized in the centers of the dots. The ground-state energy level is shifted down with descending interdot barrier thickness (see figure 3).

When the interdot barrier becomes thinner the binding energy level goes down and the antibinding level goes up on the energy scale. In the first excited state one of the electrons is in the binding orbital and the other in the antibinding orbital. The sum of the single-electron energies for the first excited state is nearly independent of b (see figure 3) since the energy shifts of binding and antibinding energy levels nearly cancel. In the absence of the interaction the second excited energy level is degenerate with respect to the spin of the electron pair. The wavefunctions for both degenerate states can be written as

$$\Psi(\mathbf{r}_1, \mathbf{r}_2) = \frac{1}{\sqrt{2}}(\psi_a(\mathbf{r}_1)\psi_b(\mathbf{r}_2) \pm \psi_a(\mathbf{r}_2)\psi_b(\mathbf{r}_1)), \tag{10}$$

where $+$ corresponds to the spin-singlet and $-$ to the spin-triplet. These wavefunctions may be expressed in terms of the single-dot wavefunctions

$$\Psi_{\mathrm{ot}}(\mathbf{r}_1, \mathbf{r}_2) = \frac{1}{\sqrt{2}}(\psi_1(\mathbf{r}_1)\psi_2(\mathbf{r}_2) - \psi_1(\mathbf{r}_2)\psi_2(\mathbf{r}_1)), \tag{11}$$

for the odd triplet and

$$\Psi_{\mathrm{os}}(\mathbf{r}_1, \mathbf{r}_2) = \frac{1}{\sqrt{2}}(\psi_1(\mathbf{r}_1)\psi_1(\mathbf{r}_2) - \psi_2(\mathbf{r}_2)\psi_2(\mathbf{r}_1)), \tag{12}$$

for the odd singlet. The wavefunction for the spin-triplet is plotted in figure 4(f) and for the spin-singlet in figure 4(j).

We see that for self-assembled dots in the spin-triplet state electrons occupy opposite dots. The antisymmetry of the wavefunction by itself does not strictly forbid electrons in the triplet state from occupying the same dot. Electrons may stay in the same dot but in different orbitals. The absence of double occupancy observed in figure 4(f) is due to the very high-energy distance between the ground-state and the first excited state for a single self-assembled dot. For planar dots the probability of finding electrons in the same dot is lower than for ground-state, but it is not zero [5]. On the other hand for the excited singlet non-zero values are allowed only at the diagonal ($z_1 = z_2$, both the electrons occupy the same dot).

The wavefunction for both the odd triplet and the odd singlet states changes sign under point inversion with respect to the symmetry center of the system $(z_1, z_2) = (5, 5)$ nm. The spin-triplet is antisymmetric with respect to inversion through the $z_1 = z_2$ line, which corresponds to an interchange of the particles (see figure 4(f)). The corresponding plot for the spin-singlet is invariant with respect to this operation (see figure 4(j)).

In the second excited state for the non-interacting pair both the electrons are in the antibinding orbitals. This state is the spin-singlet with even total parity, i.e. it has the same symmetry as the ground-state. The wavefunction is

$$\Psi_3(\mathbf{r}_1, \mathbf{r}_2) = \psi_a(\mathbf{r}_1)\psi_a(\mathbf{r}_2), \tag{13}$$

or in terms of the single-dot wavefunctions

$$\Psi_3(\mathbf{r}_1, \mathbf{r}_2) = \tfrac{1}{2}\left(\psi_1(\mathbf{r}_1)\psi_1(\mathbf{r}_2) + \psi_2(\mathbf{r}_1)\psi_2(\mathbf{r}_2) - \psi_1(\mathbf{r}_1)\psi_2(\mathbf{r}_2) - \psi_2(\mathbf{r}_1)\psi_1(\mathbf{r}_2)\right). \tag{14}$$

Similarly as for the ground-state both electrons have equal probability to be in the same or in opposite dots (see figure 4(n)).

Let us now turn our attention to the interacting system. The solid and dashed lines in figure 3 show the lowest energy levels for interacting electrons for spin-singlets and spin-triplets, respectively. The third column of plots in figures 4(c), (g), (k), (o) show the wavefunctions for interacting electrons and $b = 6$ nm. This column of plots should be compared to the second one (figures 4(b), (f), (j), (n)) discussed above, which corresponds to the same b but with the interaction switched off. We see a clear correspondence between pairs of wavefunctions with and without the electron–electron interaction (see figures 4(b) and (c), (f) and (g), (j) and (k), (n) and (o)). When the interaction is included, for the ground-state (figure 4(c)) the two maxima on the antidiagonal of the plot—corresponding to separated electrons—increase at the expense of the two maxima at the diagonal of the plot.

The wavefunctions of the lowest triplet and the first excited singlet are only slightly influenced by the interaction (compare figures 4(f), (g) and (j), (k)). Wavefunctions are not affected by the interaction since in the low-energy subspace spanned by ψ_1 and ψ_2 single-electron wavefunctions there are no extra combinations allowed having the required symmetry. The interaction lifts the degeneracy of the odd singlet and the odd triplet. The triplet becomes the lowest excited state in the presence of the interaction (see figure 3).

In contrast to the odd energy levels the interaction significantly changes the wavefunctions of the even energy levels: the ground-state and the third excited state. Both these states are singlets so the mixing does not perturb neither the spatial nor the spin symmetry. In the wavefunction of the third excited state (the first excited singlet state of even parity—figure 4(o)) we notice an opposite tendency in the electron localization to the one observed in the ground-state. The electrons in this state are more probably found in the same dot. This is a consequence of the orthogonality of this state to the ground-state, which is of the same spatial and spin symmetry. The reaction of the ground-state and the third excited state to the interaction is, in fact, due to the mixing of the non-interacting wavefunctions Ψ_0 and Ψ_3 by the electron–electron interaction.

The extent to which the non-interacting states Ψ_0 and Ψ_3 are mixed by the interaction depends on the ratio of the tunnel coupling energy (difference in the single-electron binding and antibinding energy levels) and the electron–electron interaction energy. For $b = 6$ nm the interaction energy (in the ground-state it is equal to $\simeq$13.7 meV) is comparable to the spacing between the binding and antibinding energy levels ($\simeq$9.1 meV). The wavefunctions for the interacting electrons at the barrier thickness of $b = 3$ nm are presented in figures 4(a), (e), (i), (m). For $b = 3$ nm the ground-state interaction energy and the binding–antibinding energy level splitting are equal to $\simeq$16.7 and $\simeq$47.9 meV, respectively. In fact, the wavefunctions are only slightly affected by the interaction. We notice that in the ground-state the maxima on the antidiagonal are only slightly higher than the ones on the diagonal (see figure 4(a)). The same applies for the third excited state figure 4(m).

The wavefunctions in the weak coupling limit (i.e. $b = 11$ nm) are presented in the last column of figure 4. In the ground-state (see figure 4(d)) we find along the diagonal only a residual presence of two maxima. The ground-state wavefunction in the weak interaction limit can be written as

$$\Psi = \frac{1}{\sqrt{2}}(\Psi_0 - \Psi_3) = \frac{1}{\sqrt{2}}(\psi_1(\mathbf{r}_1)\psi_2(\mathbf{r}_2) + \psi_1(\mathbf{r}_1)\psi_2(\mathbf{r}_2)), \tag{15}$$

while the wavefunction of the excited even-parity singlet is

$$\Psi = \frac{1}{\sqrt{2}}(\Psi_0 + \Psi_3) = \frac{1}{\sqrt{2}}(\psi_1(\mathbf{r}_1)\psi_1(\mathbf{r}_2) + \psi_2(\mathbf{r}_1)\psi_2(\mathbf{r}_2)). \tag{16}$$

In the state described by equation (15) both electrons occupy different dots, while in the state corresponding to the wavefunction equation (16) both electrons are in the same dot.

Note that for the weak coupling case the probability density for the ground-state (lowest spin-singlet—figure 4(d)) approaches the one for the first excited state (lowest spin-triplet—figure 4(h)). Consequently the energies of these two states become degenerate at large b (see figure 3). The two excited spin-singlet states—the one of the odd parity (figure 4(h)) and the other of the even parity (figure 4(p)) also correspond to the same probability density distribution and the corresponding energy levels become degenerate for vanishing tunnel coupling at large b (see figure 4). Note that the energy of

the degenerate ground-state decreases with b, while the energy of the degenerate excited state at large b is independent of the barrier thickness (figure 3). In the degenerate excited state both electrons occupy the same dot so the distance to the other (empty one) is irrelevant. For separated electrons the energy decreases with b. In the infinite b limit the ground-state energy for interacting electrons decreases to the ground-state energy for non-interacting electrons.

The inset to figure 3 shows the exchange energy (taken as an energy difference of the lowest triplet and lowest singlet states) as function of b for interacting (solid line) and non-interacting (dashed line) electrons. The exchange energy tends to zero when the electrons become separated into the different dots. Then, according to the discussion given above, only the electron distribution and not the spatial symmetry determines the energy of the state. In both, the lowest singlet and the lowest triplet states the separation of the electrons is enhanced by the interaction: hence the decrease in the exchange energy obtained for interacting electrons at larger b. For smaller values of b the interdot tunnel coupling effects are dominant and the interaction has a negligible effect on the exchange energy.

3.3. Exchange interaction when the electric field is oriented vertically

Figure 5 shows the wavefunctions of the four lowest energy states when an electric field is applied parallel to the axis of the dots for $b = 6$ nm (for the corresponding wavefunctions in the absence of the field see figure 4(c), (g), (k), (o)). The corresponding energy levels are displayed in figure 6(b). In the ground-state, already for $F = -12$ kV cm^{-1} the probability of finding both electrons in the lower dot is nearly zero (compare figure 5(b) with figure 4(c) for $F = 0$). For a larger electric field of $F = -50$ kV cm^{-1} (figure 5(a)) the electrons in the ground-state both become localized in the upper dot. For $F \gg 0$ both electrons in the ground-state occupy the lower dot, where the electric field potential is zero, hence no dependence on F is observed for the ground-state at the positive F side. On the other hand the ground-state energy at $F \ll 0$ decreases linearly with F (see figure 6(b)).

The lowest triplet energy level has a linear dependence on F on both sides of the $F = 0$ (see the dashed line in figure 6(b)). For the negative F the slope of this dependence is half that of the ground-state. The reason is that in the triplet state at strong $|F|$ one of the electrons becomes localized in the lower dot where the electrostatic potential is taken to be zero and the slope is only due to the other electron that remains in the upper dot (see figures 5(c), (e)). Note, that a similar F-dependence is found for the first excited singlet state outside the small F range. In the second excited singlet state both electrons occupy the dot in which the electric potential is largest (see figures 5(g), (h)).

From non-degenerate perturbation theory we know that the dependence of the energy on the perturbation is linear when the wavefunctions are not modified by the perturbation. Curvature (non-zero second derivative) of the energy levels on F is only observed when the electron distribution is changed by the field. In figure 6(b) we notice that the lowest triplet energy

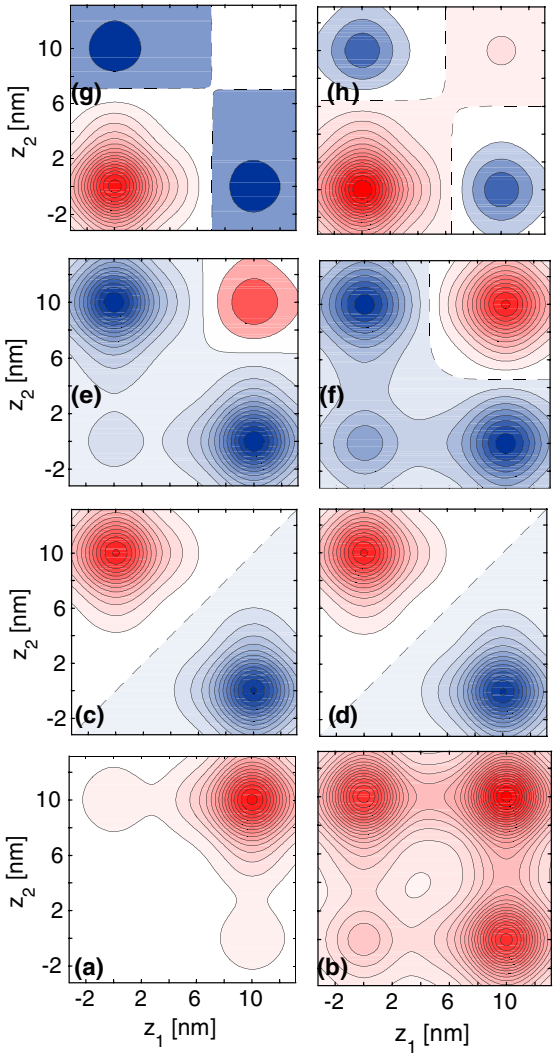

Figure 5. The same as figure 4 but for $b = 6$ nm for two different values of the electric field.

level is linear with F in the entire electric field range shown in figure 6(b) except near $F = 0$. Its wavefunction does not react to the field (see figures 5(c), (d) as well as figure 4(k)), because in the triplet state the transfer of the electrons from one dot to the other is blocked by the Pauli exclusion principle.

Figure 6(b) shows that the energies of the singlet states are nonlinear functions of F within the range of small electric fields. The electric field leads to an avoided crossing of these three energy levels, to mixing of the corresponding wavefunctions and associated transfers of the charge between the two dots. No avoided crossing is observed for the lowest triplet state. In the low-energy part of the spectrum the lowest triplet has no partner of the same spin symmetry to mix with, hence its linear dependence on F.

For the barrier thickness of $b = 11$ nm the avoided crossing between the singlet states are so narrow that with the energy scale in figure 6(c) they appear effectively as crossings of energy levels (see figure 6(c) and compare it to figure 6(b) for $b = 6$ nm). The exchange energy for $b = 2$, 6 and 11 nm is displayed in figure 6(d) as function of the electric

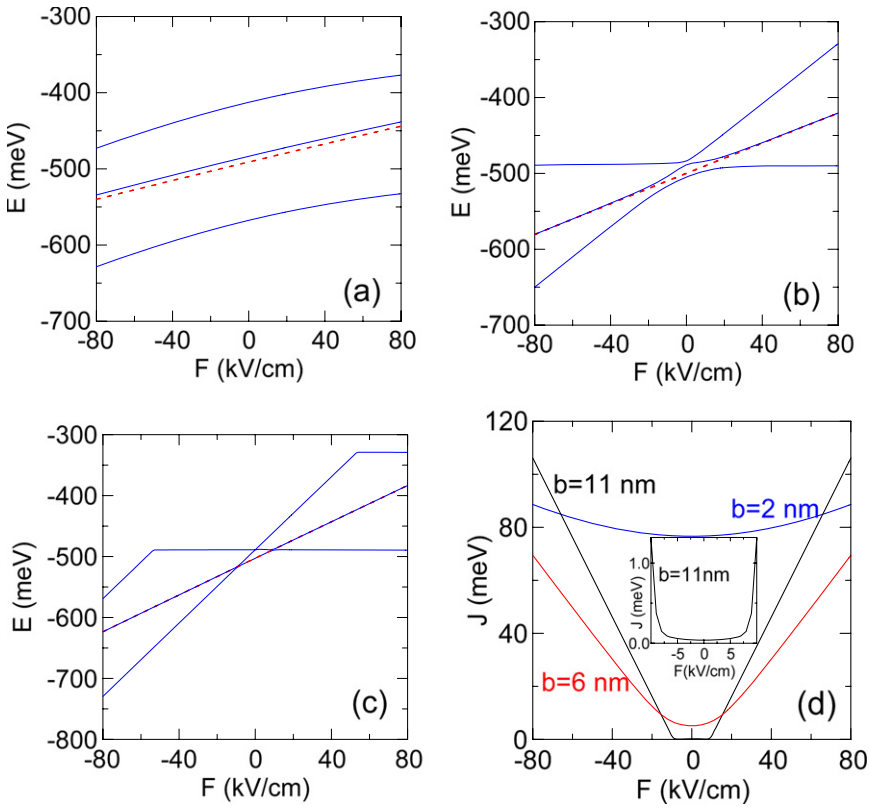

Figure 6. (a)–(c) Four lowest energy states for the electron couple in a pair of perfectly aligned quantum dots separated by a barrier thickness of $b = 2$, 4 and 11 nm for the electric field oriented along the growth direction. The zero of the electrostatic potential is taken in upper/lower dot. A positive field pushes the electrons up/down. Solid blue curves show the spin-singlet and the red dashed curve the spin-triplet energies. (d) shows the exchange energy as function of the electric field for $b = 2$ nm (blue curve) $b = 6$ nm (red curve) and $b = 11$ nm (black curve). The inset shows the exchange energy for $b = 11$ nm for electric fields close to zero.

field. For $b = 11$ nm the exchange energy is nearly zero for $F \in (-10, 10)$ kV cm^{-1} (see inset). It increases linearly with F when the near crossing of singlet states occurs in figure 6(b). The linear increase occurs when in the lowest singlet state both electrons occupy the same dot, while in the lowest triplet state the electrons occupy different dots. For $b = 6$ nm the exchange energy is a smooth function of F. The minimum value of the exchange energy occurs for $F = 0$. When an electric field is applied to the system the triplet state does not react to the field. On the other hand, in the singlet state the electrons start to occupy the deeper dot. As a consequence, when the electric field is applied the singlet state lowers its energy with respect to the triplet state, hence the minimum of the exchange energy at $F = 0$. A similar minimum is also observed for the strongly coupled dots (see the curve for $b = 2$ nm in figure 6(d)). This minimum is now much shallower, since the reaction of the singlet state to the field is reduced by the strong interdot tunnel coupling. In this electric field range the double dot with $b = 2$ nm appears as a single potential cavity.

Figure 7 shows the effects of (i) non-perfect alignment, and (ii) when there is a difference in the depth of the dots on the exchange energy for an electric field oriented in the growth direction. The red dashed curve was obtained for identical dots but with the axes of the dots shifted by about $s = 3$ nm along the x axis. The non-perfect alignment results in a reduced electron tunnel coupling, hence the reduction of exchange energy with respect to the case of perfect alignment (black solid curve in figure 7). The blue dotted curve in figure 7 represents the exchange energy that is obtained for perfectly

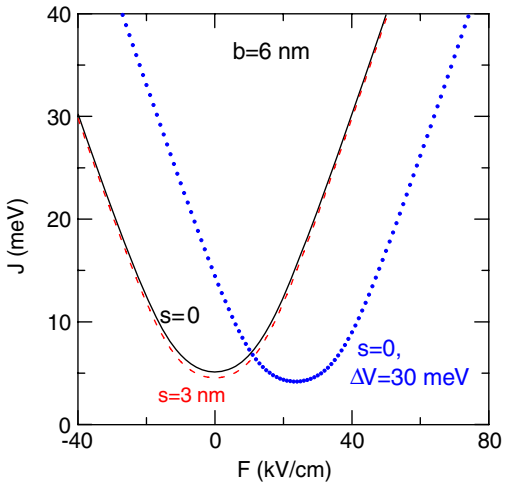

Figure 7. Exchange energy for an electron pair in a double dot with interdot barrier thickness of $b = 6$ nm in a vertical electric field. The solid black line shows the case of identical perfectly aligned ($s = 0$) dots. The dashed red curve shows the result for identical dots that are shifted by $s = 3$ nm. The dotted curve corresponds to aligned dots with the lower one deeper by 30 meV.

aligned but non-identical dots. The upper dot is assumed deeper by 30 meV. In the absence of the field the asymmetry of the dot confinement leads to a strong enhancement of the exchange energy. The reason is that both electrons in the singlet state are allowed to occupy the deeper dot which is forbidden for the triplet through the Pauli exclusion principle. The asymmetry effect is reduced for positive F, which favors the lower dot and compensates for the asymmetry in the depths of the two dots. In the singlet state a nearly equal occupancy of both dots is obtained near $F = 22$ kV cm^{-1}, for which the exchange interaction is weakest.

3.4. Lowest singlet and triplet states for an electric field perpendicular to the growth axis

As long as the electric field is applied in the vertical direction the effect of the non-perfect alignment is simply to reduce the tunnel coupling between the dots. Only when the electric field is oriented perpendicular to the growth direction has the non-perfect alignment a qualitative effect on the spectrum. In figure 8 we show the ground-state and the first excited energy levels for identical dots that are shifted by $s = 5$ nm along the x-direction. We apply a weak electric field of $F = 20$ kV cm^{-1} which we rotate in the (x, y) plane. The electric field direction is $\mathbf{F} = F(\sin(\phi), \cos(\phi), 0)$. For ideally aligned dots ($s = 0$) rotation of the electric field vector has practically no influence on the energy spectrum. In figure 8 we see that the ground-state energy is minimal when the electric field is aligned with the x axis, i.e. with the direction of the shift between the dots. The ground-state wavefunction is localized in the dot that is shifted down in energy due to the electric potential. The oscillation of the excited state energy with ϕ is in anti-phase with the one in the ground-state energy. When the ground-state wavefunction occupies the deeper dot the excited state wavefunction goes necessarily to the shallower dot by the orthogonality constraint. Note that the average of the two energy levels is independent of the electric field orientation (see the dashed curve in figure 8). The curves presented in figure 8 were obtained in the Gaussian basis, while the crosses in figure 8 show the results from the finite difference approach. The finite difference method and the Gaussian basis approach produce very similar results. In the Gaussian basis we apply four centers forming a cross in the $x-y$ plane. The granularity of the Gaussian basis is not visible in the results for the rotated electric field, although in principle one could be concerned about this issue.

In figure 9(a) we display the three lowest singlet energy levels (solid blue curves) and the lowest triplet energy level (red dashed curve) for a pair of electrons confined in two vertically coupled dots as were considered in figure 8. We see that for non-zero s the ground-state energy is minimal when the electric field is parallel to the x axis, i.e., when the field is aligned with the direction of the shift between the dots. The ground-state energy is maximal for the electric field perpendicular to the shift between the centers of the dots. The evolution of the two-electron ground-state energy follows the trend set by the single-electron ground-state (figure 8).

Figure 10 shows the charge density in the lowest singlet (lower panels ((a), (b))) and the lowest triplet (upper panels

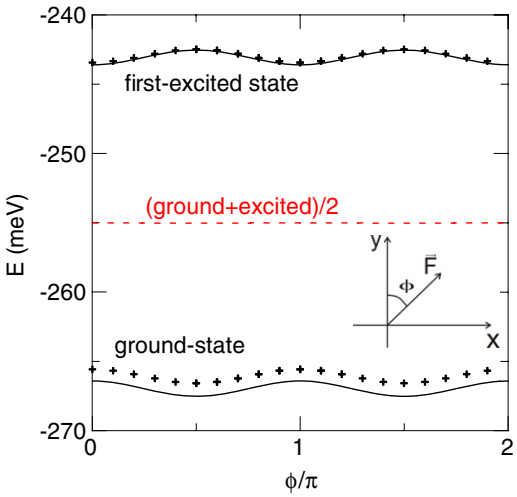

Figure 8. Solid lines show the ground-state and the first excited energy levels for a single electron in a double dot with interdot barrier $b = 6$ nm and axes of the two identical dots shifted by $s = 5$ nm as a function of the orientation of a weak electric field of $F = 20$ kV cm^{-1} that is perpendicular to the growth direction. For $\phi = \pi/2$ (parallel) and $\phi = 3\pi/2$ (antiparallel) the field is aligned along the x axis (i.e. the direction of the shift between the dots) (see the inset). The dashed curve shows the arithmetic average of the two energy levels. The crosses indicate the results of a finite difference approach.

((c), (d))) for the electric field oriented along the y-direction (left panels) and along the x-direction (right panels). For the electric field oriented in the y-direction (figures 9(a), (c)) each of the dots in both the singlet and the triplet contains a single electron. When the field is redirected to the x-direction (figures 9(b), (d)), the charge in the lower dot, preferred by the electric potential, is increased in the singlet state, which lowers the ground-state energy. In the triplet state we notice no transfer of the electron charge to the lower dot, which is forbidden by the Pauli exclusion principle. Consequently, the energy of the triplet state is independent of the electric field orientation (see figure 9(a)). This can also be understood as due to the fact that the lowest triplet wavefunction is predominantly built up of an antisymmetrized product of the single-electron wavefunction of the ground-state and the single-electron wavefunction of the first-excited-state. The sum of those single-electron energies is independent of the electric field orientation (see figure 8). Moreover, in the triplet the electron–electron interaction energy should also be independent of ϕ since no redistribution of the electron charge between the dots is observed in the triplet state (see figure 10).

The thick gray line in figure 9(a) shows the exchange energy as function of the electric field orientation. It is maximal for the electric field oriented parallel to the x axis, when the singlet lowers its energy by double occupancy of the dot that is shifted to lower energy by the electric field. The double occupancy of the deeper dot is blocked for the triplet state.

Figure 9(b) shows the effect of the electric field rotation when one of the dots of figure 9(b) is made deeper by 20 meV. Similarly, as in the case of identical dots, the triplet energy

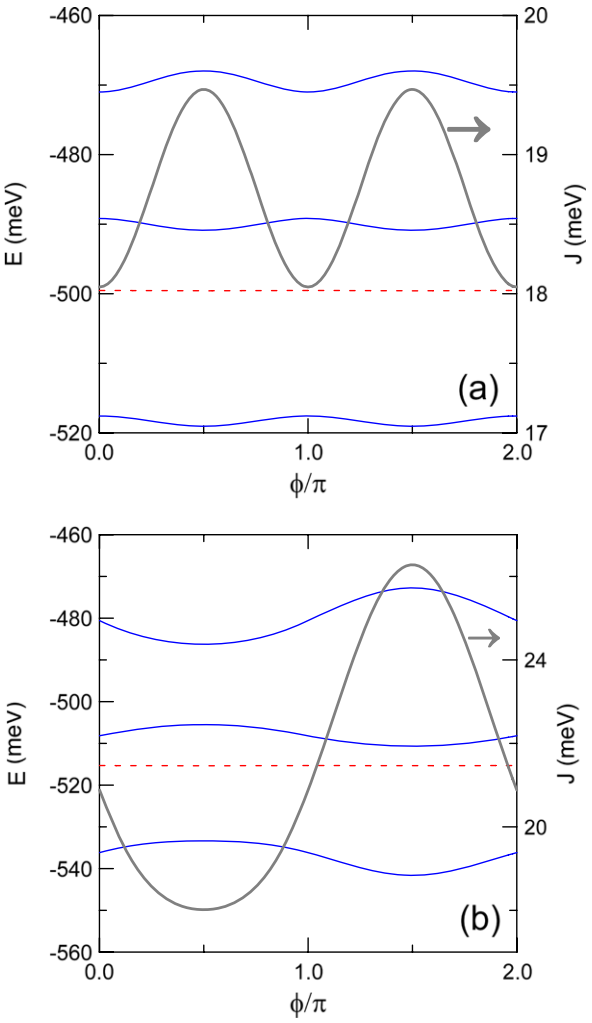

Figure 9. (a) Solid blue and dashed red curves show the four lowest energy levels of an electron pair as function of the orientation in the (x, y) plane of a weak electric field $F = 20$ kV cm^{-1}. The two identical dots are shifted by $s = 5$ nm and are separated by a barrier with thickness of $b = 6$ nm. The energy levels are referred to the left axis. The thick gray curve shows the exchange energy and is referred to the right axis. (b) The same as (a) but where the lower dot is deeper by 20 meV. For $\phi = 3\pi/2$ the electric force acting on the electrons is directed towards the deeper dot. In both cases the exchange energy is equal to the spacing between the lowest solid and the lowest dashed curve.

does not depend on the electric field orientation. For $\phi = \pi/2$ the electric field potential compensates for the non-equal confinement depths of the dots. This results in a maximal ground-state energy. The asymmetry in the depth of the dots is increased for $\phi = 3\pi/2$, which coincides with the minimum of the ground-state energy. Variation of the ground-state energy is directly translated into the ϕ dependence of the exchange energy. Note, that for non-identical dots the amplitude of the variation of the exchange energy with ϕ is much larger as compared to the case of identical dots (cf figures 9(a) and (b)).

3.5. Stack of three identical dots

A contour plot of the wavefunctions for the lowest singlet and triplet energy levels of a non-interacting pair of electrons

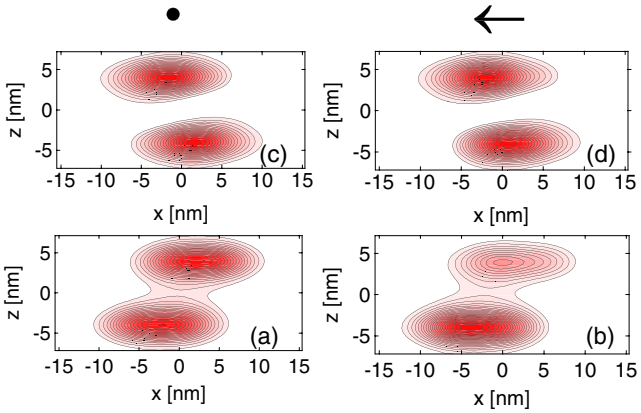

Figure 10. Charge density for the ground-state ((a), (b)) (lowest singlet) and the first excited state ((c), (d)) (lowest triplet) for two identical dots displaced by $s = 5$ nm in a weak electric field of 20 kV cm^{-1} directed within the (x, y) plane. In ((a), (c)) the electric field is oriented perpendicular to the x axis. In ((b), (d)) the electric force for electrons is directed to the left (see the arrow).

in a stack of three dots are displayed in figure 11 in the (z_1, z_2)—plane for $y_1 = x_1 = y_2 = x_2 = 0$. The dots are assumed perfectly aligned, identical and separated by an interdot barrier of thickness $b = 6$ nm. The ground-state (see figure 11(a)) wavefunction possesses 9 maxima, corresponding to both electrons localized in one of the three dots. The global maximum of the wavefunction occurs for both electrons in the central dot. In the triplet state only 6 extrema of the wavefunction are obtained; the electrons never occupy the same dot, hence the wavefunction extrema at the diagonal are missing. Of the 6 extrema the largest ones are associated with electrons occupying opposite ends of the stack, in spite of the fact that the interaction is neglected in this plot. However, the probability to find one electron in the central dot and the other in an adjacent one is also significant (see the extrema when one of the coordinates is equal to zero and the other is ± 10 nm).

The wavefunctions for the lowest energy singlet and triplet states in the presence of the interaction and for the same parameters of the external potential are displayed in figures 12(a) and (e), respectively. The interaction enhances the maxima that correspond to electrons localized at opposite ends of the stack. In the lowest singlet plot the local extrema at the diagonal of the plot are visibly decreased (compare figures 12(a) and 11(a)).

The effect of the vertical electric field on the energy spectrum of the stack is shown in figure 13. Similarly, as in the case of two dots, the ground-state reacts to the electric field more readily than the lowest triplet state which leads to an enhancement of the exchange interaction. In contrast to the double-dot case the energy of the triplet state is not a linear function of the electric field. The difference to the double-dot case is that the triplet wavefunction is modified by the external electric field which results in the non-linearity. The lowest triplet wavefunctions for non-zero F are presented in figures 14(c), (d). When an electric field is applied, the electrons in the triplet state tend to occupy only the middle and uppermost dot within the stack. For stronger F in the singlet both electrons occupy the uppermost dot figures 14(a), (b).

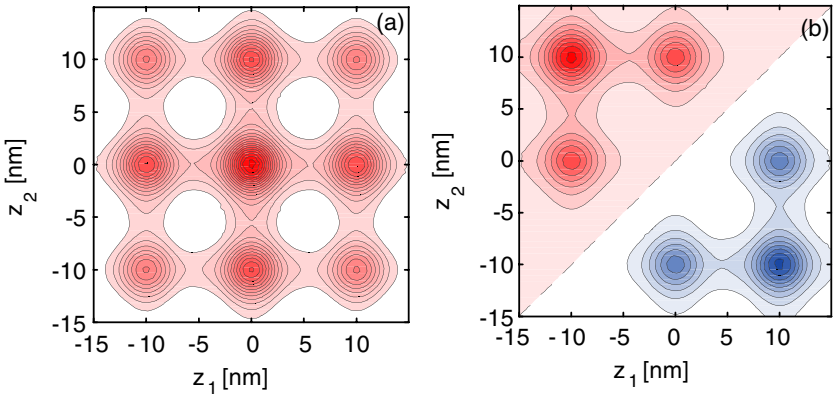

Figure 11. The same as figure 4 for a pair of non-interacting electrons, but now in a stack of three dots that are equally spaced by a barrier with thickness of $b = 6$ nm, (a) corresponds to the ground-state (lowest singlet) and (b) to the first excited state (lowest triplet).

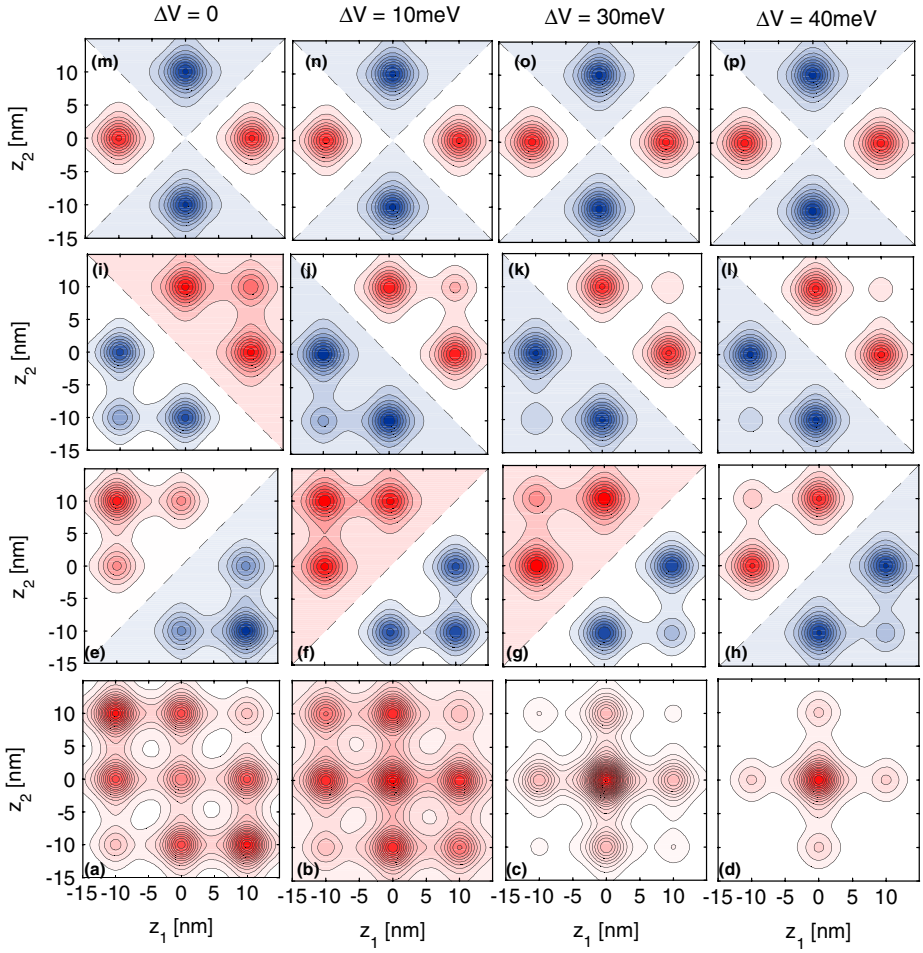

Figure 12. The same as figure 11 but now for interacting electrons. In the first column (a), (e), (l), (m) the dots are identical. In subsequent columns the central dot is deeper by $\Delta V = 10$, 30 and 40 meV. The lowest row ((a)–(d)) corresponds to the ground-state, ((e)–(h)) to the lowest energy triplet, ((i)–(l)) to the first excited singlet, and ((m)–(p)) to the first excited triplet.

3.6. Vertical stack of three dots with deeper a central dot

The wavefunctions of two lowest energy singlets and two lowest energy triplets are displayed in figure 12 for increasing depth of the central dot ΔV. As ΔV grows the central dot is occupied by a single electron in the triplet state, and by both electrons in the singlet state. The first excited singlet plotted in figures 12(i)–(l) has odd parity. It possesses a nodal surface on the antidiagonal of the plot. Similarly as in the triplet state only one electron occupies the central dot as ΔV increases. The first excited triplet state has even parity. It possesses two nodal surfaces at both the antidiagonal and the diagonal of the

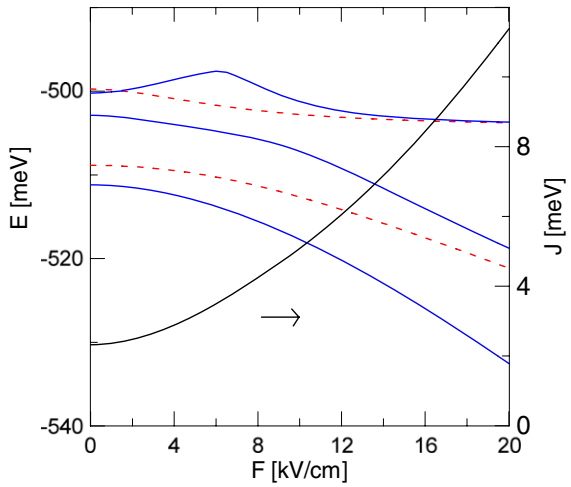

Figure 13. Singlets (blue solid) and triplet (red dashed) energy levels for an electron pair in three identical dots separated by barriers of width $b = 6$ nm as a function of an electric field along the growth direction. The black solid curve shows the exchange energy (referred to the right axis).

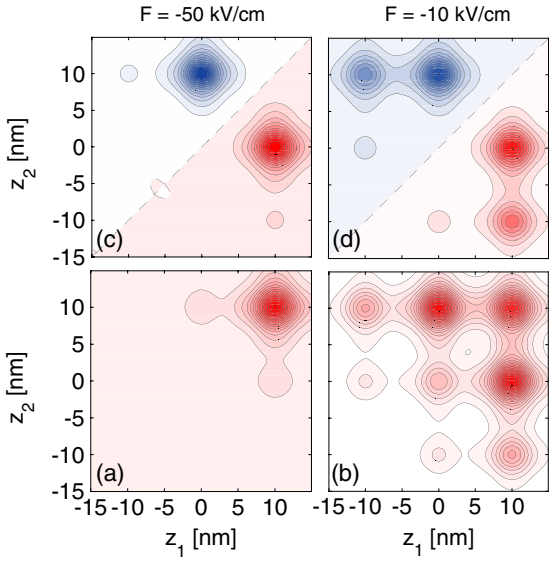

Figure 14. Wavefunctions of the lowest singlet ((a), (b)) and lowest triplet ((c), (d)) states in an external electric field directed along the stack of three identical dots.

plot. Its wavefunction does not react to changes in the depth of the central dot. Note, that the probability density of all the three excited states tend to the same shape with increasing depth of the central dot.

The energy levels as function of ΔV are displayed in figure 15. We note that the energy levels of the three excited states become degenerate at large ΔV, in accordance with the increasing similarity of the probability densities. The energy of the even-parity triplet state is exactly linear in ΔV (rigid wavefunction effect). The exchange energy is increased by a factor of 9 when ΔV is changed from 0 to 36 meV.

In the stack with a deeper central dot the lowest-energy triplet is nearly degenerate with respect to the parity. The

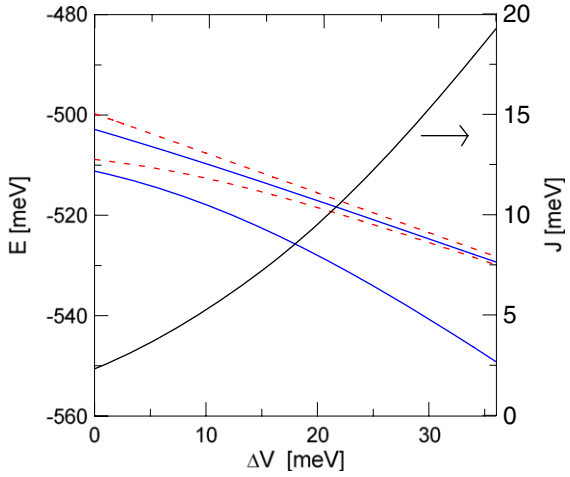

Figure 15. The same as figure 13 but as function of the depth of the central dot.

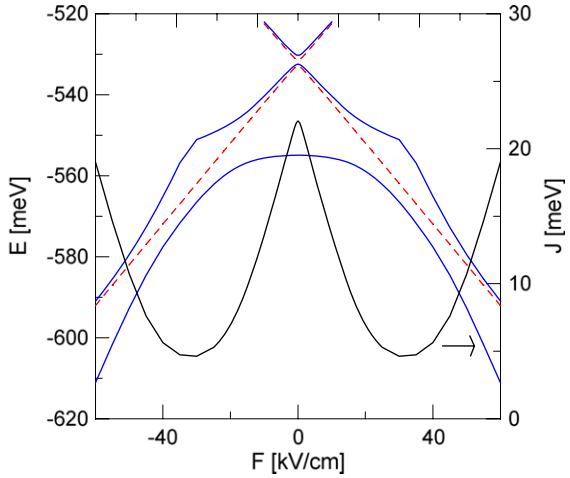

Figure 16. The same as figure 13 but for a central dot which is deeper by $\Delta V = 40$ meV with respect to the others.

electric field easily mixes these two triplets, and therefore the reaction of the lowest triplet to the electric field is quite prompt. Figure 13 shows the energy spectrum as function of the electric field. Mixing of the triplets is visible as a narrow avoided crossing of dashed curves near $F = 0$. Outside of the avoided crossing area the triplet state becomes a linear function of F. The wavefunction of the lowest energy triplet state in the presence of an external electric field is displayed in figures 14(c), (d).

The dependence of the lowest singlet (ground-state) state on the electric field is weaker. The electric field tends to remove electrons from the central dot which is the deepest (see figure 14), hence the retarded reaction with respect to the triplet state, which results in a maximum of the exchange energy at $F = 0$ (in the stack of identical three and two dots $F = 0$ corresponds to the minimum of the exchange energy). J has two minima near $F = \pm 30$ kV cm^{-1}. It starts to increase with $|F|$ when the two electrons in the singlet occupy the extreme dot of the stack, which is not allowed for the triplet.

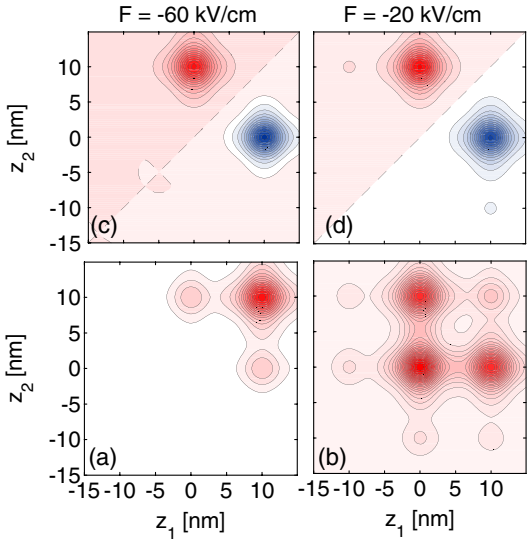

Figure 17. The same as figure 14 but for a central dot that is deeper by $\Delta V = 40$ meV.

4. Discussion

In vertically coupled self-assembled quantum dots the low-energy part of the spectrum consists of three singlets and a single triplet state. We demonstrated that both the electron–electron interaction and the external electric field leads to mixing of the singlet energy levels while the modification of the triplet spatial wavefunction due to both the electron–electron interaction and the electric field is negligible, since the triplet has no low-energy counterpart to mix with. The Pauli exclusion principle which prevents electrons with a symmetric spin wavefunction to occupy the same spatial position in the case of small quantum dots results in a separation of electrons into different dots. On the other hand electrons in the singlet react promptly to the external electric field tending to occupy both the dots favored by the electric potential. The different dependence of the singlet and triplet to the electric field in double dots results in an enhancement of the exchange interaction. For identical self-assembled dots an electric field parallel to the axis of the stack always enhances the exchange energy. On the other hand for non-identical dots the electric field enhances or reduces the exchange energy depending on its orientation. The exchange energy is reduced by a weak electric field oriented in a way that compensates the non-equal confinement of the dots and it is enhanced for the opposite orientation increasing the asymmetry of the confinement potential. For the first orientation, the exchange energy starts to increase with the value of the field only when the shallower dot is made lower in the energy by the electric potential. This results in a occurrence of a minimum of the exchange energy for a non-zero F.

For a stack of three identical dots the triplet wavefunction is no longer independent of the electron–electron interaction and the external electric field. The dependence of the exchange energy in the case of three identical dots on the external electric field is similar to the double-dot system. We demonstrated that it can be strongly enhanced by making the central dot deeper than the top and bottom dots of the stack due to the Pauli exclusion principle. Moreover, increasing the depth of the central dot leads to a degeneracy of the lowest triplet states and to an increase the energy spacing between the ground-state and the lowest excited singlet. For that reason, in contrast to the double-dot system, the dependence of the triplet state on the external field is larger than for the singlet. The exchange interaction is therefore strongest for $F = 0$. The exchange energy has minima at both electric field orientations before it eventually starts to increase. This increase occurs when the electric field localizes both singlet electrons in the extreme dots of the stack.

5. Summary and conclusions

In summary we investigated an electron pair in a double and triple vertical stack of self-assembled quantum dots using the configuration-interaction approach and a three-dimensional model of the system. Effects of the non-perfect alignment of the dots and unequal depths of the dots within the stack were discussed. Particular attention was paid to the manipulation of the electrons by an external electric field oriented along the axis of the stack. We discussed the effects of the interaction and the electric field on the singlet and triplet energy levels as well as on the exchange interaction. As long as the electric field is oriented along the axis of the stack the non-perfect alignment of the dots results in a reduction of the interdot tunnel coupling which typically amounts in a reduction of the exchange energy. Non-perfect alignment only has a qualitative effect on the exchange energy when the electric field is oriented perpendicular to the axis of the stack.

The presented results indicate that the exchange energy is sensitive to the details of the confinement of the coupled dot system and can be conveniently controlled by the external electric field. In particular for weakly coupled dots the external electric field can be used to switch on the exchange interaction, which in the absence of the field is zero due to the perfect separation of electrons in different dots. The values of the exchange energy obtained for the stacked dots are by two orders of magnitude larger than the ones obtained for lateral electrostatic dots.

Acknowledgments

This work was supported by the EU Network of Excellence: SANDiE and the Belgian Science Policy (IAP).

References

[1] Reimann S M and Manninen M 2002 *Rev. Mod. Phys.* **74** 1283
[2] Burkard G, Loss D and DiVincenzo D P 1999 *Phys. Rev.* B **59** 2070
Burkard G, Seelig G and Loss D 2000 *Phys. Rev.* B **62** 2581
[3] Hu X and Das Sarma S 2000 *Phys. Rev.* A **61** 062301
[4] Harju A, Siljamäki S and Nieminen R M 2002 *Phys. Rev. Lett.* **88** 226804
[5] Szafran B, Peeters F M and Bednarek S 2004 *Phys. Rev.* B **70** 205318

[6] Pedersen J, Flindt C, Mortensen N A and Jauho A-P 2007 *Phys. Rev.* B **76** 125323
[7] Saraiva A L, Calderon M J and Koiller B 2007 *Phys. Rev.* B **76** 233302
[8] Häusler W and Kramer B 1993 *Phys. Rev.* B **47** 16353
Szafran B, Peeters F M, Bednarek S, Chwiej T and Adamowski J 2004 *Phys. Rev.* B **70** 035401
Mueller E J 2005 *Phys. Rev.* B **72** 075322
Fogler M M and Pivovarov E 2006 *J. Phys.: Condens. Matter* **18** L7
Sako T and Diercksen G H F 2008 *J. Phys.: Condens. Matter* **20** 155202
[9] Loss D and DiVincenzo D P 1998 *Phys. Rev.* A **57** 120
[10] Hanson R, Willems van Beveren L H, Vink I T, Elzerman J M, Naber W J M, Koppens F H L, Kouwenhoven L P and Vandersypen L M K 2005 *Phys. Rev. Lett.* **94** 196802
[11] Stopa M, Vidan A, Hatano T, Tarucha S and Westervelt R M 2006 *Physica* E **34** 616
[12] Melnikov D V, Leburton J-P, Taha A and Sobh N 2006 *Phys. Rev.* B **74** 041309(R)
Zhang L-X, Melnikov D V and Leburton J-P 2006 *Phys. Rev.* B **74** 205306
Zhang L-X, Melnikov D V and Leburton J-P 2007 *IEEE Trans. Nanotechnol.* **6** 250
[13] Kwasniowski A and Adamowski J 2008 *J. Phys.: Condens. Matter* **20** 215208
[14] Moskal S, Bednarek S and Adamowski J 2007 *Phys. Rev.* A **76** 032302
[15] Krenner H J, Clark E C, Nakaoka T, Bichler M, Scheurer C, Absteiter G and Finley J J 2006 *Phys. Rev. Lett.* **97** 076403
[16] Stinaff E A, Scheibner M, Bracker A S, Pomonarev I V, Korenev V L, Ware M E, Doty M F, Reinecke T L and Gammon D 2005 *Science* **311** 636
Krenner H J, Clark E C, Nakaoka T, Bichler M, Scheurer C, Abstreiter G, Finley J J and Scheurer C 2006 *Phys. Rev. Lett.* **97** 076403
Bracker A S, Scheibner M, Doty M F, Stinaff E A, Pomonarev I V, Kim J C, Whitman L J, Reinecke T L and Gammon D 2006 *Appl. Phys. Lett.* **89** 233110
Scheibner M, Yakes M, Bracker A S, Ponomarev I V, Doty M F, Hellberg C S, Whitman L J, Reinecke T L and Gammon D 2008 *Nat. Phys.* **4** 291
[17] Degani M H, Farias G A and Farinas P F 2006 *Appl. Phys. Lett.* **89** 152109
Degani M H and Maialle M Z 2007 *Phys. Rev.* B **75** 115322
Chu W and Zhu J L 2006 *Appl. Phys. Lett.* **89** 053122
Xu D, Zhao N and Zhu J L 2008 *J. Phys.: Condens. Matter* **20** 045204
Szafran B, Barczyk E, Peeters F M and Bednarek S 2008 *Phys. Rev.* B **77** 115441
Mlinar V and Peeters F M 2007 *J. Mater. Chem.* **17** 3687
[18] Szafran B, Peeters F M and Bednarek S 2007 *Phys. Rev.* B **75** 115303
[19] Bellucci D, Rontani M, Troiani F, Goldoni G and Molinari E 2004 *Phys. Rev.* B **69** 201308
[20] Davies K T, Flocard H, Kreger S and Weiss M S 1980 *Nucl. Phys.* A **341** 112